Title

Ocean-atmosphere forcing of centennial hydroclimate variability in the Pacific Northwest

Authors

Byron A. Steinman, Department of Meteorology and Earth and Environmental Systems Institute, The Pennsylvania State University, University Park, PA 16802-5013, USA.

Mark B. Abbott, Department of Geology and Planetary Science, University of Pittsburgh, Pittsburgh, PA 15260-3332, USA.

Michael E. Mann, Department of Meteorology and Earth and Environmental Systems Institute, Department of Geosciences, The Pennsylvania State University, University Park, PA 16802-5013, USA.

Joseph D. Ortiz, Department of Geology, Kent State University, Kent, OH 44242, USA.

Song Feng, Department of Geosciences, University of Arkansas, Fayetteville, AR 72701, USA.

David P. Pompeani, Department of Geology and Planetary Science, University of Pittsburgh, Pittsburgh, PA 15260-3332, USA.

Nathan D. Stansell, Department of Geology and Environmental Geosciences, Northern Illinois University, DeKalb, IL 60115, USA

Lesleigh Anderson, U.S. Geological Survey, Denver Federal Center, Denver, CO 80225, USA

Bruce P. Finney, Department of Geosciences, Department of Biological Sciences, Idaho State University, Pocatello, ID 83209-8072, USA.

Broxton W. Bird, Department of Earth Sciences, Indiana University-Purdue University Indianapolis, Indianapolis, IN 46202, USA.

Corresponding Author: Byron A. Steinman, Department of Meteorology and Earth and Environmental Systems Institute, The Pennsylvania State University, University Park, PA 16802-5013, USA (bas56@psu.edu).

This article has been accepted for publication and undergone full peer review but has not been through the copyediting, typesetting, pagination and proofreading process which may lead to differences between this version and the Version of Record. Please cite this article as doi: 10.1002/2014GL059499

Abstract

Reconstructing centennial timescale hydroclimate variability during the late Holocene is critically important for understanding large-scale patterns of drought and their relationship with climate dynamics. We present sediment oxygen isotope records spanning the last two millennia from 10 lakes, as well as climate model simulations, indicating that the Little Ice Age was dry relative to the Medieval Climate Anomaly in much of the Pacific Northwest of North America. This pattern is consistent with observed associations between the El Niño Southern Oscillation (ENSO), the Northern Annular Mode and drought as well as with proxy-based reconstructions of Pacific ocean-atmosphere variations over the past 1000 years. The large amplitude of centennial variability indicated by the lake data suggests that regional hydroclimate is characterized by longer-term shifts in ENSO-like dynamics, and that an improved understanding of the centennial timescale relationship between external forcing and drought conditions is necessary for projecting future hydroclimatic conditions in western North America.

Key Points

Lake sediment isotope records exhibit coherent centennial timescale variability

The Little Ice Age was dry in much of the Pacific Northwest

Climate model simulations support drought patterns evinced by lake sediment data

1. Introduction

The response of regional hydroclimate to external forcing is the subject of considerable scientific interest due to its potential impact on global water availability. Analyses of observational data [*Dettinger et al*., 1998; *Wang et al.*, 2006; *Wise*, 2010] indicate that interannual- to decadal-scale drought patterns in the American West are largely controlled by the interplay of the El Niño Southern Oscillation (ENSO) and the Northern Annular Mode (NAM) (Figs. 1, A1), which climate models and paleoclimate proxy data suggest are affected by external forcing [*Cook et al*., 2004; *Seager et al*., 2008; *Graham et al*. 2011]. The timing and magnitude of drought in much of the American West during the Little Ice Age (LIA) (defined by the Intergovernmental Panel on Climate Change as ~1450-1850 AD) and the Medieval Climate Anomaly (MCA) (defined as ~900-1300 AD) have been reconstructed using a variety of proxy data [e.g. *Cook et al*., 2004, 2010; *Steinman et al*., 2012], but significant questions remain about the magnitude, spatial coherence, and causes of drought in the greater Pacific Northwest, particularly on multi-decadal to centennial timescales. It is likely, for example, that mean state hydroclimatic shifts lasting multiple centuries occurred in the past due to synoptic climate (e.g. ENSO/NAM) responses to external (i.e. solar and volcanic) forcing, and that such shifts could occur in the future with profound socioeconomic implications. Investigating the temporal patterns and driving mechanisms of such lower frequency climate change is therefore of critical importance to the development of sustainable water resource management strategies. To this end, we analyze paleoclimate proxy data including 10 lake sediment oxygen isotope (δ^{18}O) records [*Stevens et al*., 2006; *Anderson et al*., 2007; *Stevens and Dean*, 2008; *Shapley et al*., 2009; *Nelson et al*., 2011; *Steinman et al*., 2012] and tree ring records [*Cook et al.*, 2004, 2010] from western North America as well as climate model simulation results (Auxiliary Material). The resulting synthesis of

paleoclimate data provides insights into the influence of Pacific and Atlantic ocean-atmosphere variability and external forcing on decadal to millennial scale climate change.

2. Regional Climate

ENSO and the Pacific Decadal Oscillation (PDO) influence precipitation amounts and temperature in the Pacific Northwest by modifying the strength and position of the Aleutian Low and North Pacific high pressure systems and the westerly winds that deliver water vapor to the continental interior in late fall and winter. Wet periods often occur during the negative phase of ENSO (i.e. La Niña, as defined by the Nino3/3.4 index) when the Aleutian Low weakens (or shifts to a more westerly position) and promotes a more northerly storm track, and vice versa [*Dettinger et al*., 1998; *Wise*, 2010] (Figs. 1, A1). The NAM also influences climate in North America, with positive NAM phases characterized by a greater pressure difference between extra-tropical high and low pressure centers and a stronger mid-latitude jet stream that produces more zonal westerly winds [*Wang et al*., 2006]. Positive NAM phases often produce wetter conditions in the Pacific Northwest, with a stronger influence at higher latitudes. Precipitation patterns in this region (Fig. A2) vary from north to south with the majority of rain/snowfall occurring during the warm season and cold season, respectively.

3. Methods and Results

To account for chronologic uncertainties, a Monte Carlo–based randomization method [*Marcott et al*., 2013] was applied to the 10 lake sediment records (Fig. A3; Auxiliary Material). 100 individual age model realizations were produced for each record by randomly selecting dates from the 2σ uncertainty range of each age control point. To account for variability in the isotopic composition of precipitation, isotopic anomalies in the open lake (Jellybean, Lime) records were subtracted from proximal closed lake series (i.e. Marcella, Castor, and Renner) [*Anderson et al*., 2007; *Steinman et al*., 2012]. The resulting Δδ records

(Castor-Lime, Renner-Lime, Marcella-Jellybean) represent changes in the oxygen isotopic composition ($\delta^{18}O$) of lake water corrected for the influence of variability in $\delta^{18}O$ of precipitation. Each lake record realization was interpolated at a 10-year time step (the average sampling interval) (Table A1) and standardized by mean centering and dividing each mean-centered value by the standard deviation of the series (Fig. 2). The standardized (z-scores) series were then averaged to produce the regional records (i.e. Eastern and Western; Figs. 2C, 2F). The 2σ uncertainty range for each stacked record is defined by the standard deviation of the 100 series at each time step. The Palmer Drought Severity Index (PDSI) data (Version 2a) from the grid points corresponding with each lake location were standardized and averaged in the same manner but were not interpolated. T-tests establish the significance of the difference between mean values from the LIA and MCA in each of the 100 realizations of the Eastern and Western Stacked series (Fig. A4). We did not conduct t-tests on the tree ring data because the difference between mean values from the MCA and LIA are negligible (e.g. the difference in the Western PDSI stack is <0.02).

Average z-score values from the LIA are greater than values from the MCA in 7 of the 8 closed lake records (Fig. 2), indicating drier conditions. The Washington lakes (Castor-Lime, Renner-Lime) exhibit the largest magnitude difference between the MCA and LIA; whereas the Rocky Mountain records (Cleland, Foy, Jones, Crevice) exhibit the smallest difference between the two time periods. T-test comparisons reveal that the difference between the mean LIA and MCA values in the Western z-score composite (Fig. 2, A4) is significant ($p<0.05$), and that the difference between the two time periods in the Eastern z-score series is also likely significant (although with a larger uncertainty range during the MCA).

4. Discussion and Conclusions

Lake hydrologic and isotopic responses to climate change depend on lake size (e.g.

volume and surface area) and the proportion of water lost though groundwater outflow, overflow and evaporation. Hydrologically closed lakes lose the majority of water through evaporation and are more isotopically enriched relative to open lakes, which lose water primarily through non-fractionating outflows such as overflow and groundwater seepage. Closed lakes that lose all water through evaporation reach the limit of isotopic enrichment, and open lakes that lose no (or very little) water through evaporation maintain an isotopic composition similar to that of meteoric water [Steinman and Abbott, 2013]. Physical modeling studies of small, surficially closed lake systems at multi-decadal resolution indicate that higher $\delta^{18}O$ values reflect lake isotopic responses to drier conditions, reduced groundwater inflow rates, and warmer temperatures [*Shapley et al*., 2009; *Steinman et al*., 2010; *Steinman et al.*, 2012]. Lower $\delta^{18}O$ values result from the opposite set of conditions. Reddening of the isotopic signal in sediment from small lake systems (i.e. similar to those studied here) does not affect average isotopic values on multi-decadal to centennial timescales due to short lake-water residence times. In contrast, large lakes can exhibit a reddened isotopic response, due to much larger equilibration times, that leads to mean isotopic values that are not contemporaneous with hydroclimatic conditions [*Benson et al*., 2002]. Model simulations of the isotopic and hydrologic mass balance of Castor Lake demonstrate a strong isotopic sensitivity to winter (November-February) precipitation and lesser control by precipitation and temperature in all other seasons [*Steinman et al*., 2012]. Other model simulations indicate that low frequency hydroclimatic variations produce water isotopic changes in groundwater throughflow lakes, and that the seasonality of precipitation can also affect water and sediment isotopic composition [*Shapley et al*., 2009]. In general, modeling studies [e.g. *Shapley et al*., 2009; *Steinman et al*., 2010] indicate that lake sensitivity to seasonal climate forcing is dependent on the local climatic and hydrologic setting, and that all lakes with considerable water loss through evaporation are sensitive to

hydroclimate variability regardless of the season in which it occurs. On this basis, the large (greater than 0.5 ‰) differences between the LIA and MCA in several of the records (e.g. Castor, Marcella, and Crevice) (Fig. A3) are thought to have occurred due to appreciable changes in net precipitation/evaporation balance [*Anderson et al*., 2007; *Steinman et al*., 2012].

Inferred colder temperatures during the LIA [*Galloway et al*., 2011] cannot explain higher isotope values in lake sediment from this time. This is because temperature decreases produce lower evapotranspiration rates and greater water availability, a scenario that leads to positive hydrologic fluxes, lower water and sediment $\delta^{18}O$ values and is inconsistent with the lake records. Furthermore, subtracting the open-lake isotope anomalies from the Castor, Renner, and Marcella records removed the influence of changes in the $\delta^{18}O$ of precipitation, as well as the effect of varying temperatures on equilibrium carbonate mineral fractionation, from the closed lake $\delta^{18}O$ series [*Anderson et al*., 2007; *Steinman et al*. 2012]. A possible limitation of the $\Delta\delta$ method is that open-lakes could also exhibit isotopic responses to large hydroclimate anomalies that affect evaporation rates (e.g. exceptionally warm summers). However, the low magnitude of variability in the Lime and Jellybean records indicates that such responses either did not occur, or were short lived, over the past 2000 years. Thus, changes in net precipitation are likely the principal control on lake hydrology and the corresponding sediment oxygen isotope values presented here.

The composite lake sediment oxygen isotope data indicate that drier conditions prevailed during the LIA and that the MCA was relatively wetter (Fig. 2). This implies that substantial variability occurred in the mean state of the Pacific ocean-atmosphere system on centennial timescales. This result is consistent with a multi-proxy PDO reconstruction [*Mann et al*., 2009] that provides insight into North Pacific responses to low-frequency ENSO dynamics and signifies generally negative (cool phase) PDO conditions during and prior to

the MCA and a more positive (warm phase) PDO thereafter (Fig. 3). This PDO pattern is in turn consistent with inferred warmer (cooler) central and Western Pacific Ocean temperatures resulting from a La Niña- (El Niño-) like Pacific Ocean mean state. Tropical Pacific sea surface temperature (SST) reconstructions from the West Pacific warm pool and the Niño3.4 region support this assessment [*Cobb et al.*, 2003; *Verdon and Franks*, 2006; *Oppo et al*., 2009; *Li et al*. 2011].

The lake isotope trend toward more positive values (i.e. drier conditions) during the past millennium is consistent with long term trends in proxy records of Pacific and Atlantic ocean-atmosphere variability (Fig. 3), suggesting that the observed interannual to decadal relationship between ENSO and winter precipitation-evaporation balance in the Pacific Northwest (Fig. 1) operates on centennial timescales. The drying trend is evident in the lake sediment data until the past ~200 years when the Washington and Yukon records diverge (Auxiliary Material). Instrumental data indicate that winter precipitation-evaporation responses to ENSO/NAM in northwestern British Columbia and the southern Yukon are opposite those of inland Washington and the Rocky Mountain sites. The similar LIA/MCA trend in the Marcella Lake data relative to those of the Washington records may therefore be due to large warm season hydroclimate anomalies that (Figs. 1, A1). Given the dynamical connection between ENSO and the PDO [*Verdon and Franks*, 2006], shifts in mean tropical Pacific Ocean conditions may also have resulted from more frequent and persistent El Niño and La Niña anomalies during the LIA and the MCA, respectively. Cumulatively, such changes in ENSO frequency and/or magnitude likely affected average Pacific Northwest hydroclimate, particularly in the cold season when ENSO teleconnections are strongest [*Dettinger et al*., 1998; *Wise*, 2010].

Experiments using the National Center for Atmospheric Research (NCAR) Community Atmosphere Model (CAM) support the hydroclimate patterns evinced by the

lake data (Auxiliary Material). Two sets of experiments were conducted in which (i) global and (ii) tropical mean temperature anomalies from the MCA were used to force the model (Fig. A5, Tab. A2). The simulations reproduced reduced cold season precipitation during the LIA relative to the MCA in the Pacific Northwest (Figs. 4, A6). Furthermore, the largest LIA precipitation anomalies are observed in Washington and decrease inland toward the Rocky Mountains and to the north, a pattern that is consistent with the lake $\delta^{18}O$ data. Additional similarities include a difference between LIA and modern precipitation amounts that is larger than the difference between mean MCA and modern precipitation, and warm season precipitation anomalies during the MCA and LIA that are opposite in sign of the cold season anomalies (Figs. A7, A8). The use of global rather than tropical SSTs to force the model produced larger precipitation changes, but the spatial patterns of the two tests are largely consistent. This suggests that the tropical Pacific is the primary driver of North American precipitation anomalies in the model simulations.

Comparison of the low-frequency variability evident in lake sediment and tree-ring based Palmer Drought Severity Index (PDSI) reconstructions reveals several disparities (Figs. 3, A9; Tab. A3). Across all of the regions, average reconstructed PDSI values from the MCA and LIA are ±0.15, or well within the range of near-normal conditions of ±0.5 as defined by the PDSI. This implies that hydroclimate has not varied substantially on centennial timescales over the last 1000 years and is in stark contrast to the considerable centennial-scale hydroclimatic variations indicated by the composite lake sediment isotope records. This finding may be a result of different seasonal sensitivities of the lake and tree-ring proxies [*St. George et al*., 2010; *St. George and Ault*, 2014], and the limited ability of some tree-ring records to capture multi-decadal climate variations on longer (multi-centennial to millennial) timescales [*Esper et al*., 2011]. It has been shown, for example, that in much of the Pacific Northwest tree-ring growth is most strongly influenced by soil moisture content

during the growing season; whereas, lake isotope values are strongly influenced by cold season precipitation [*St. George et al*., 2010; *Steinman et al.*, 2012].

Changes in extra-Pacific synoptic dynamics with different impacts on climate during different seasons could explain the disparity between the tree ring and lake sediment records. For example, multi-proxy data from the Atlantic basin indicate a weakening of the North Atlantic Oscillation (NAO) over the last two millennia (Fig. 3) [*Trouet et al.*, 2009; Auxiliary Material]. Observational data indicate that when the NAM/NAO is in a positive phase (Jan-Mar average) and ENSO is in a negative phase (Jun-Nov average), warm season precipitation-PET amounts (at a lag of 10 months from the prior June) are lower on average in the southern Pacific Northwest [*McAfee and Russell*, 2008] and greater in much of the northern Pacific Northwest (Fig. A1). In the CAM simulations, warm season precipitation rates are higher during the LIA and lower during the MCA in much of western North America (a pattern opposite that of the cold season) (Fig. A8). Such a hydroclimatic scenario of wetter winters with simultaneously drier summers, and vice versa, explains the apparent inconsistency between the two proxies in the Washington region, in which lakes are strongly influenced by October-March precipitation [*Steinman et al*., 2012]. This could also explain why the lake isotope records from the Rocky Mountains, which are subject to larger summer precipitation anomalies (due to a larger proportion of annual precipitation occurring during summer), do not universally exhibit a large disparity between mean isotope values from the MCA and LIA. Nevertheless, the lake data indicate that perturbations in the mean state of the tropical Pacific forced larger century timescale hydroclimatic shifts in much of the Pacific Northwest than can be inferred from the tree-ring data.

Modeling [*Mann et al*., 2005; *Graham et al*., 2011] and proxy data [*Mann et al*., 2009; *Marchitto et al*., 2010; *Ersek et al*., 2012] comparisons show links between mean tropical Pacific Ocean conditions and radiative forcing [*Crowley et al*., 2000] that provide

insight into potential future responses of the ocean-atmosphere system to greenhouse gas forcing. Studies of proxy data sets including tree rings [*Cook et al*., 2004, 2010] and speleothems [*Asmerom et al*., 2007] suggest connections between inferred solar activity maxima, La Niña-like conditions in the tropical Pacific and reduced water availability in the American Southwest. Lake sediment data from the Pacific Northwest reveal an opposite pattern in which centennial periods of lower solar activity correspond with dryness, and vice versa, similar to the north-south antiphased pattern of drought that occurs on annual to decadal timescales in response to ENSO (Figs. 1, 4). Proxy data therefore reveal a climatic response that is consistent with the hypothesized "ocean dynamical thermostat" mechanism in which increases in radiative forcing produce a cooling of the eastern tropical Pacific [*Mann et al*., 2005; 2009; *Marchitto et al*., 2010]. The large magnitude of centennial variability revealed by the lake sediment data implies that the climate system is characterized by longer-term shifts in ENSO-like dynamics and further, that a better understanding of Pacific and Atlantic Ocean-atmosphere responses to external climate forcing is necessary for projecting future hydroclimatic conditions in western North America.

Acknowledgments

This research was funded by the following US National Science Foundation grants (acknowledging authors): AGS-1137750 (B.A.S.), EAR-0902200 (M.B.A.)**,** ATM-0902133 (M.E.M.), EAR-0902753 (J.D.O.), and AGS-1103316 (S.F.). We thank Jeremy Moberg, Chris Helander, Daniel Nelson, Jason Addison, and Janet Slate. Lake sediment isotope data are available on the National Climatic Data Center Paleoclimatology website: http://www.ncdc.noaa.gov/data-access/paleoclimatology-data/datasets

References

Anderson, L., M. B. Abbott, B. P. Finney, and S. J. Burns (2007), Late Holocene moisture balance variability in the southwest Yukon Territory, Canada. *Quaternary Sci. Rev.*, *26*, 130–140.

Asmerom, Y., V. Polyak, S. Burns, and J. Rassmussen (2007), Solar forcing of Holocene climate: New insights from a speleothem record, southwestern United States. *Geology*, *35*(1), 1–4.

Benson, L., M. Kashgarian, R. Rye, S. Lund, F. Paillet, J. Smoot, C. Kester, S. Mensing, D. Meko, and S. Lindström (2002), Holocene multidecadal and multicentennial droughts affecting northern California and Nevada. *Quaternary Sci. Rev.*, *21*, 659–682.

Cobb, K. M., C. D. Charles, H. Cheng, and R. L. Edwards (2003), El Niño/Southern Oscillation and tropical Pacific climate during the last millennium. *Nature*, *424*, 271–276.

Cook, E. R., C. A. Woodhouse, C. M. Eakin, D. M. Meko, and D. W. Stahle (2004), Long-term aridity changes in the western United States. *Science*, *306*, 1015–1018.

Cook, E. R., R. Seager, R. R. Heim Jr., R. S. Vose, C. Herweijer, and C. Woodhouse (2010), Megadroughts in North America: Placing IPCC projections of hydroclimatic change in a long-term palaeoclimate context. *J. Quaternary Sci.*, *25*(1), 48–61.

Crowley, T. J. (2000), Causes of climate change over the past 1000 years. *Science*, *289*, 270–277.

Dettinger, M. D., D. R. Cayan, H. F. Diaz, and D. M. Meko (1998), North-south precipitation patterns in western North America on interannual-to decadal timescales. *J. Clim.*, *11*, 3095–3111.

Ersek, V., P. U. Clark, A. C. Mix, H. Cheng, and R. L. Edwards (2012), Holocene winter climate variability in mid-latitude western North America. *Nat. Commun.*, *3*, 1219.

Esper, J., D. C. Frank, M. Timonen, E. Zorita, R. J. S. Wilson, J. Luterbacher, S. Holzkämper, N. Fischer, S. Wagner, D. Nievergelt, A. Verstege, and U. Büntgen (2011), Orbital forcing of tree-ring data. *Nature Clim. Change*, *2*, 862–866.

Galloway, J. M., A. M. Lenny, and B. F. Cumming (2011), Hydrological change in the central interior of British Columbia, Canada: Diatom and pollen evidence of millennial-to-centennial scale change over the Holocene. *J. Paleolimnol.*, *45*, 183–197.

Graham, N. E., C. M. Ammann, D. Fleitmann, K. M. Cobb, and J. Luterbacher (2011), Support for global climate reorganization during the ‘‘Medieval Climate Anomaly’’. *Clim. Dyn.*, *37*, 1217–1245.

Li, J., S.-P. Xie, E. R. Cook, G. Huang, R. D'Arrigo, F. Liu, J. Ma, and X.-T. Zheng (2011), Interdecadal modulation of El Niño amplitude during the past millennium. *Nature Clim. Change*, *1*, 114–118.

Mann, M. E., M. A. Cane, S. E. Zebiak, and A. Clement (2005), Volcanic and solar forcing of the tropical Pacific over the past 1000 years. *J. Clim.*, *18*, 447–456.

Mann, M. E., Z. Zhang, S. Rutherford, R. S. Bradley, M. K. Hughes, D. Shindell, C. Ammann, G. Faluvegi, and F. Ni (2009), Global signatures and dynamical origins of the Little Ice Age and Medieval Climate Anomaly. *Science*, *326*, 1256–1260.

Marchitto, T. M., R. Muscheler, J. D. Ortiz, J. D. Carriquiry, and A. v. Geen (2010), Dynamical response of the tropical Pacific Ocean to solar forcing during the early Holocene. *Science*, *330*, 1378–1381.

Marcott, S. A., J. D. Shakun, P. U. Clark, and A. C. Mix. (2013), A reconstruction of regional and global temperature for the past 11,300 years. *Science*, *339*, 1198–1201.

McAfee, S. A., and J. L. Russell (2008), Northern Annular Mode impact on spring climate in the western United States. *Geophys. Res. Lett.*, *35*, L17701.

Nelson, D. B., M. B. Abbott, B. A. Steinman, P. J. Polissar, N. D. Stansell, J. D. Ortiz, M. F. Rosenmeier, B. P. Finney, and J. Riedel (2011), A 6,000 year lake record of drought from the Pacific Northwest. *P. Natl. Acad. Sci. USA*, *108*, 3870–3875.

Oppo, D. W., Y. Rosenthal, and B. K. Linsley (2009), 2,000-year-long temperature and hydrology reconstructions from the Indo-Pacific warm pool. *Nature*, *460*, 1113–1116.

Seager, R., R. Burgman, Y. Kushnir, A. Clement, E. Cook, N. Naik, and J. Miller (2008), Tropical Pacific forcing of North American Medieval megadroughts: Testing the concept with an atmosphere model forced by coral-reconstructed SSTs. *J. Clim.*, *21*, 6175–6190.

Shapley, M. D., E. Ito, and J. J. Donovan (2009), Lateglacial and Holocene hydroclimate inferred from a groundwater flow-through lake, Northern Rocky Mountains, USA. *The Holocene*, *19*(4), 523–535.

Steinman, B. A., M. B. Abbott, M. E. Mann, N. D. Stansell, and B. P. Finney (2012), 1500 year reconstruction of precipitation in the Pacific Northwest. *P. Natl. Acad. Sci. USA*, *109*, 11619–11623.

Steinman, B. A., and M. B. Abbott (2013), Isotopic and hydrologic responses of small, closed lakes to climate variability: Hydroclimate reconstructions from lake sediment oxygen isotope records and mass balance models. *Geochim. Cosmochim. Acta*, *105*, 342–359.

Steinman, B. A., M. F. Rosenmeier, M. B. Abbott, and D. J. Bain (2010), The isotopic and hydrologic response of small, closed-basin lakes to climate forcing from predictive models: application to paleoclimate studies in the upper Columbia River basin. *Limnol. Oceanogr.*, *55*, 2231–2245.

Stevens, L. R., J. R. Stone, J. Campbell, and S. C. Fritz (2006), A 2200-yr record of hydrologic variability from Foy Lake, Montana, USA, inferred from diatom and geochemical data. *Quaternary Res.*, *65*, 264–274.

Stevens, L. R., and W. E. Dean (2008), Geochemical evidence for hydroclimatic variability over the last 2460 years from Crevice Lake in Yellowstone National Park, USA. *Quatern. Int.*, *188*, 139–148.

St. George, S., and T. R. Ault (2014), The imprint of climate within Northern Hemisphere trees. *Quaternary Sci. Rev*, *89*, 1–4.

St. George, S., D. M. Meko, and E. R. Cook (2010), The seasonality of precipitation signals embedded within the North American Drought Atlas. *The Holocene*, *20*(6), 983–988.

Trouet, V., J. Esper, N. E. Graham, A. Baker, J. D. Scourse, and D. C. Frank (2009), Persistent positive North Atlantic Oscillation mode dominated the Medieval Climate Anomaly. *Science*, *324*, 78–80.

Verdon, D. C., and S. W. Franks (2006), Long-term behavior of ENSO: Interactions with the PDO over the past 400 years inferred from paleoclimate records. *Geophys. Res. Lett.*, *33*, L06712.

Wang, X. L., H. Wan, and V. R. Swail (2006), Observed changes in cyclone activity in Canada and their relationships to major circulation regimes. *J. Clim.*, *19*, 896–915.

Wise, E. K. (2010), Spatiotemporal variability of the precipitation dipole transition zone in the western United States. *Geophys. Res. Lett.*, *37*, L07706.

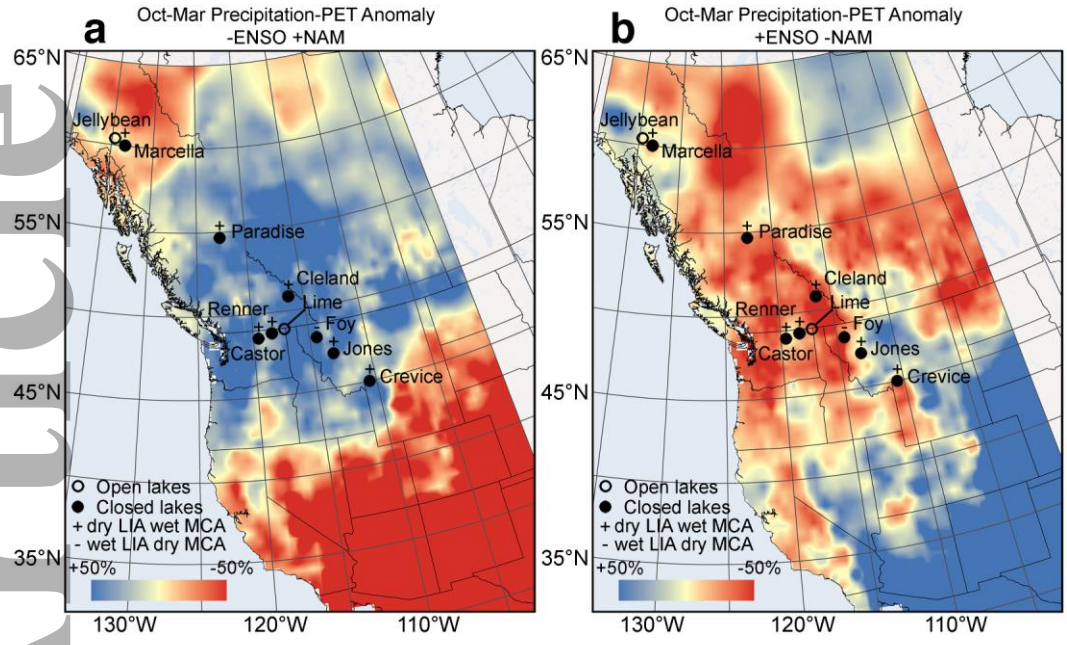

Figure 1. Average percent change in October-March precipitation minus PET (relative to total October-March precipitation) during (a) years of negative ENSO and positive NAM, and (b) vice versa (Auxiliary Material). Plus (minus) signs represent a drier (wetter) LIA relative to the MCA in the lake isotope records.

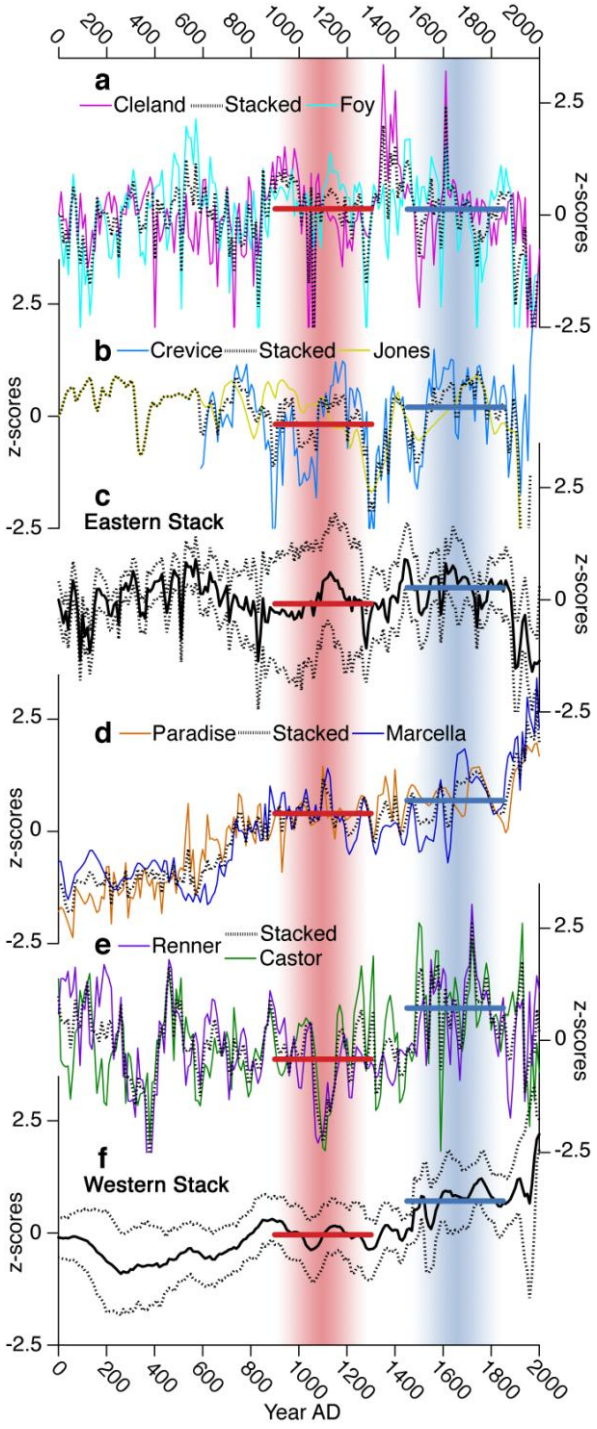

Figure 2. Sediment oxygen isotope z-scores with independent age models (Fig. A10) from (a) two of the northern sites in the Rocky Mountain (Cleland, Foy) [*Stevens et al*., 2006], (b) two of the southern sites in the Rocky Mountain (Crevice, Jones) [*Stevens and Dean*, 2008; *Shapley et al*., 2009], (c) Eastern stacked composite produced by averaging the standardized (z-score) values of the Rocky Mountain datasets (excluding Jones because of limited age

model control), (d) northern sites (Paradise, Marcella-Jellybean) [*Anderson et al*., 2007], (e) Washington sites (Renner-Lime, Castor-Lime) [*Nelson et al*., 2011; *Steinman et al*., 2012] plotted with (f) the Western stacked composite produced by averaging the standardized (z-score) values of the northern and Washington datasets. Mean values from the MCA and LIA are shown by the red and blue bars, respectively. The dashed lines in panels (c) and (f) represent the 2σ uncertainty range based on the assessment of age model uncertainty.

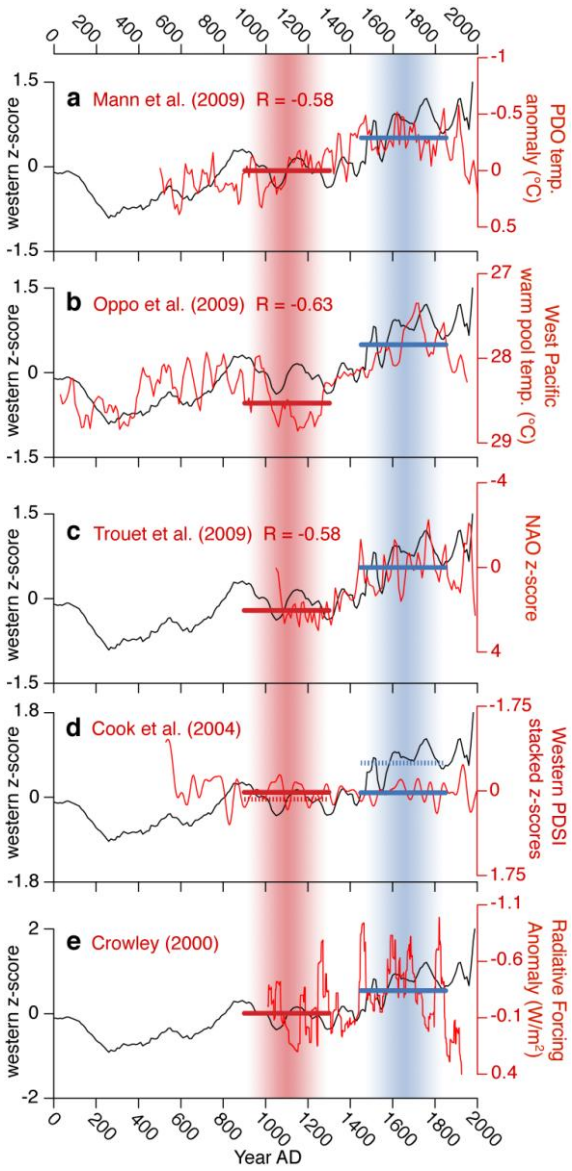

Figure 3. Western stacked (averaged z-scores) lake sediment isotope record (Fig. 2F) compared with (a) PDO temperature anomalies [*Mann et al*., 2009], (b) West Pacific warm pool temperatures [*Oppo et al*., 2009], (c) NAO z-scores [*Trouet et al*., 2009], (d) composite PDSI reconstructions from the grid points corresponding with each western lake location [*Cook et al*., 2004] (Version 2a) (50 year low pass filter), and (e) total radiative forcing anomalies [*Crowley*, 2000] (25 year moving average). PDO, West Pacific SST, and NAO data were interpolated at 10 year intervals. Correlations were calculated using 50 year moving averages of interpolated data. Mean values from the MCA and LIA are shown by the red and blue bars, respectively (lake isotope mean values in panel D are dashed).

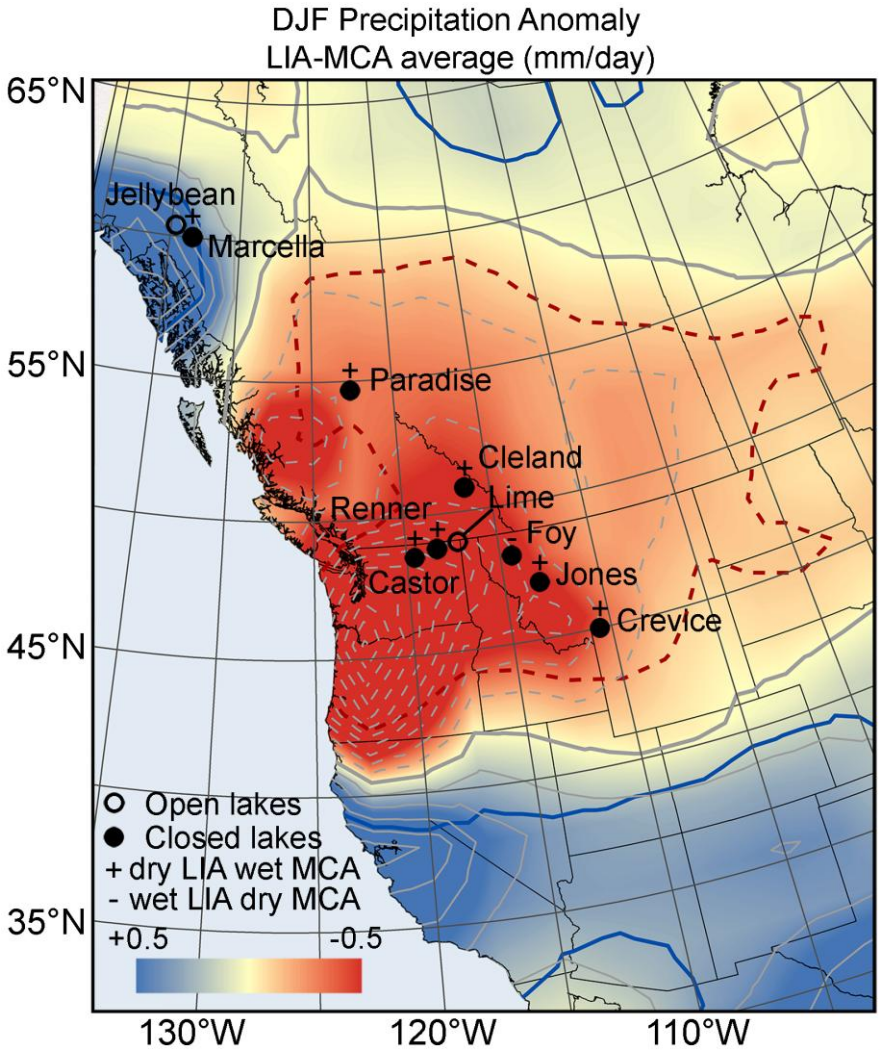

Figure 4. CAM results: the difference between simulated December-February precipitation anomalies (mm/day) forced by SSTs during the LIA (LIA_g) and MCA (MCA_g) (LIA average minus MCA average) (Tab. A2). The red and blue lines enclose regions where the precipitation differences are significant at the 95% confidence level by a two-tailed t-test. Grey contours are spaced in 0.2 mm/day intervals. The thick contour line depicts a value of 0.